

## Removable template route to metallic nanowires and nanogaps

R. Šordan,<sup>a)</sup> M. Burghard, and K. Kern

Max-Planck-Institut für Festkörperforschung, Heisenbergstrasse 1, D-70569 Stuttgart, Germany

(Received 30 May 2001; accepted for publication 23 July 2001)

A general method for the fabrication of nanowires with a thickness of  $\sim 6$  nm and width of 15–20 nm is presented. The approach is applicable to inorganic and organic materials and is demonstrated here for metallic systems. The wires are produced by ion-beam etching of a gold–palladium thin films covered by chemically modified vanadium–pentoxide nanowires as an etching mask. The two-probe room-temperature resistance of the wires is found to range between 7.8 and 18.1 k $\Omega$ . Nanogaps with a length on the order of 1 nm were created within the nanowires by breaking via electromigration. © 2001 American Institute of Physics. [DOI: 10.1063/1.1405813]

The development of nanotechnology has not only contributed to a better understanding of the fundamental properties of matter in reduced dimensions, but also has promoted the application of these materials in modern electronics. From the physical point of view, metallic nanowires (MNWs) are interesting because they exhibit a broad range of low-dimensionality effects,<sup>1–3</sup> such as ballistic conduction,<sup>4</sup> the Aharonov–Bohm effect,<sup>5</sup> conductance fluctuations,<sup>6</sup> and weak localization.<sup>7</sup> On the other hand, MNWs could be used as interconnects between highly integrated transistors in future electrical circuits, where the main goal is to decrease the number of interconnecting levels and capacitive cross talk.<sup>8</sup> Metallic nanowires also show great potential for chemical sensor applications. For example, they may be used as probes for molecules capable of adsorbing on a gold surface.<sup>9</sup> Sensors based upon metal wires of ultrasmall width and thickness are expected to exhibit high sensitivities and short response times.

The standard way to create MNWs follows an advanced electron-beam lithography (EBL) procedure.<sup>10</sup> However, for dimensions below the resolution limit of standard EBL (typically, 30 nm), an alternative approach is required. Electrochemical deposition<sup>4</sup> and shadow deposition<sup>11</sup> can surpass the resolution limit of EBL, but in the first case, the wires do not have a uniform cross section, while in the second case a special (grated) surface is required for deposition. Nanowires on a scale below 10 nm can be produced by evaporating a metal into a channel formed by etching a cleaved molecular-beam-epitaxy-grown substrate.<sup>12</sup> Another successful approach is to use appropriate nanowires as an etching mask to create metallic ones. This technique is promising because many different types of nanowires, like nanotubes<sup>13</sup> or semiconductor nanowires,<sup>14</sup> are now synthetically available. Due to their small dimensions and mechanical strength,<sup>15</sup> carbon nanotubes seem to be well suited for the etching mask technique. However, attempts made so far were unable to completely remove the nanotube mask after the etching process, and also did not lead to conducting MNWs.<sup>16</sup> In addition, variations in the size of the tubes<sup>15</sup> result in nanowires of different widths. Here, we present the application of chemically modified vanadium–pentoxide ( $V_2O_5$ ) fibers as a ver-

satile etching mask to fabricate continuous gold–palladium (AuPd) nanowires. The fibers are about 8 nm in height and sufficiently stable to protect a AuPd layer of 6 nm thickness during argon-ion-beam etching. In contrast to most other nanowires, the remaining parts of the  $V_2O_5$  template can be easily dissolved in dilute acid. The whole fabrication process is schematically represented in Fig. 1.

The chemically modified  $V_2O_5$  fibers were prepared via hydrolysis of 100  $\mu$ l of vanadium(V)oxy-tri(isopropoxide) (Ref. 17) in 20  $\mu$ l of *N*-methylformamide (NMF)/water (1/200). After mixing of the components, the solution was heated to 80 °C for 15 min. Oxide fibers with an average length of 1  $\mu$ m were obtained after aging for three weeks under ambient conditions. While hydrolysis in pure water results in unmodified  $V_2O_5$  fibers with a cross section of 1.5 nm  $\times$  10 nm, the fibers modified by the presence of NMF are thicker and wider (6–10 nm  $\times$  15–20 nm). A thin metal

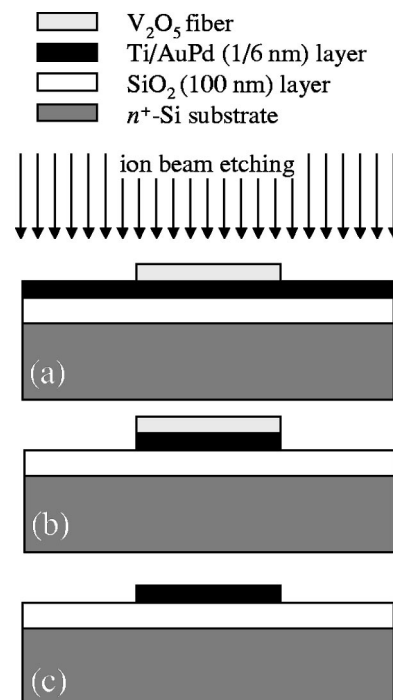


FIG. 1. Schematic illustration of the nanowire fabrication process. (a)  $V_2O_5$  fibers are employed as an etching mask on top of the thin metal layer. (b) AuPd film unprotected by the etching mask is removed by IBE. (c) Remaining parts of the  $V_2O_5$  wires are removed with a dilute acid solution.

<sup>a)</sup>Electronic mail: roman@fkf.mpg.de

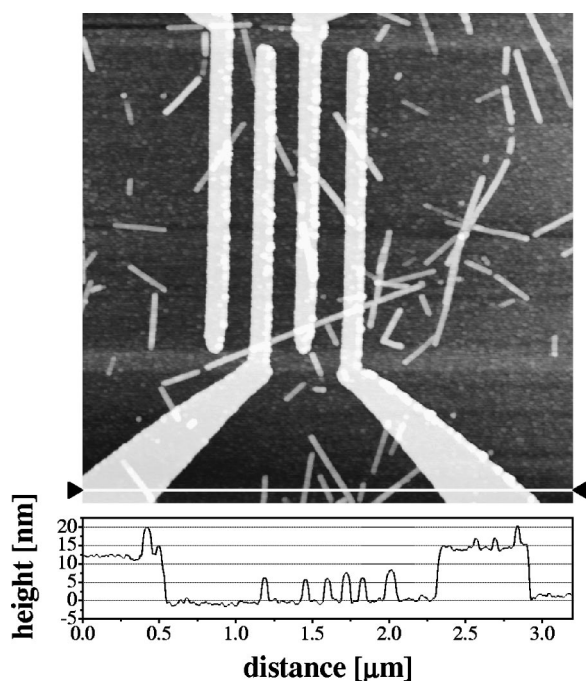


FIG. 2. Atomic-force microscopy (AFM) image of 6-nm-thick AuPd nanowires below AuPd electrodes. While the left-hand pair of electrodes is not connected, the middle pair is connected by one nanowire, and the right-hand pair by two nanowires. The AFM height profile along the marked white line is shown at the bottom of the image.

film consisting of a 1-nm-thick Ti adhesion layer and a 6-nm-thick AuPd (60/40) layer was evaporated onto a 100-nm-thick SiO<sub>2</sub> insulating layer on a Si substrate. Prior to fiber deposition, the AuPd surface was reacted with a 1 mM aqueous solution of 3-aminopropyl-dimethyl(ethoxy)silane for 2 min at room temperature. In this step, positively charged surface groups are created that serve to bind the negatively charged V<sub>2</sub>O<sub>5</sub> fibers. An appropriate density of fibers was obtained by immersing the modified substrate into the fiber solution for 10 s, followed by rinsing with pure water and blowing dry with argon. Subsequent to argon-ion-beam etching (IBE), (for 10 s with an acceleration voltage of 200 V), the remaining parts of the oxide wires were completely removed by immersion in 5% HCl solution for 15 min. To make electrical contacts, four AuPd electrodes, 15 nm in thickness and separated by 120 nm, were defined on each substrate by EBL.

An atomic-force microscopy (AFM) image of one of the investigated samples is depicted in Fig. 2. The AFM section profile along the white line at the bottom reveals that the wire heights range between 6 and 8 nm. The long wire in the lower half of the image is 1.5 μm long and 15 nm in width, as determined by scanning electron microscopy. This wire connects the three electrode lines on the right side, whereas for the left electrode pair, there exists no nanowire connection. Two-probe transport measurements were performed in air at room temperature in a bias range ±100 mV. The resistance of the left-hand electrode pair is too high to be measured, which demonstrates that the parts of the thin metal layer, which remained unprotected by the etching mask, were successfully removed. For the middle electrode pair, a resistance of 8.4 kΩ was found, while the right pair showed a smaller value of 6.4 kΩ due the presence of a second con-

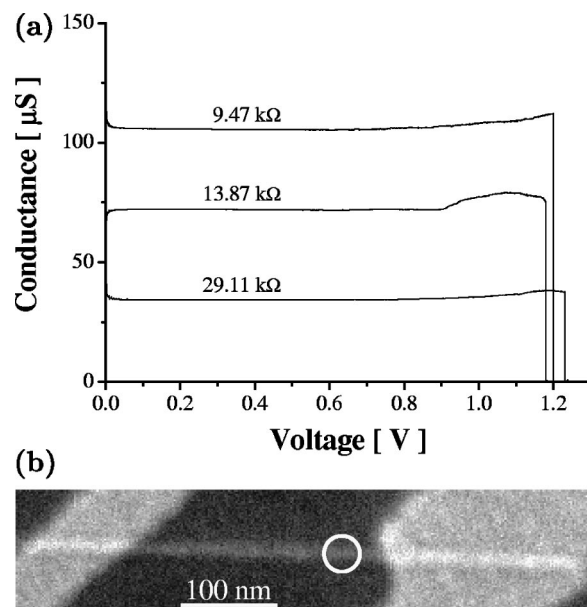


FIG. 3. (a) Breaking characteristics of three different AuPd nanowires produced in two different series. Curves are denoted by the resistance that corresponds to the flat region. (b) Scanning electron microscope (SEM) image of a nanowire after breaking. The gap is encircled. An additional SEM image taken from a different angle revealed the interruption at the same spot.

nection via the shorter wire in the upper region. The majority of the investigated single-wire connections showed a resistance in the range between 7.8 and 18.1 kΩ. Although these values are close to the resistance quantum  $h/(2e^2) = 12.9 \text{ k}\Omega$ , electrical transport in these nanowires is unlikely to be ballistic because the wires, consisting of evaporated metal, do not have an ordered crystalline structure.

Four-probe measurements were also performed under the same conditions. In all cases, the four-probe resistance was found to be between 1/3 and 1/2 of the total (two-probe) resistance. The residual resistance is due to the contact resistance between the fibers and electrodes, and the series resistance of electrodes themselves (typically, ~4 kΩ). The studied MNWs exhibit fully metallic behavior with no observable dependence of both the two- and four-probe resistances on the applied back-gate voltage (for up to ±100 V). No change of the wire resistance has been detected after their storage for several weeks. They are able to sustain voltages up to 0.8 V (corresponding to a current density of  $10^{12} \text{ A/m}^2$ ) without any apparent damage or change in resistance, but they are very sensitive to electrostatic discharge.

MNWs can be broken by electromigration which is the thermally induced motion of metal ions due to the presence of a high current density inside the structure. This process is the main cause of failure in commercial electronic circuitry,<sup>18</sup> however, it has also been used to produce nanogaps.<sup>19</sup> The main advantage of using MNWs to produce nanogaps is the possibility of creating gaps with the same cross section as the MNWs. The nanoscaled cross section of the gap may eventually allow the attachment of only one molecule between the two parts of the MNW and, therefore, the creation of a single-molecule transistor.<sup>20</sup> The breaking characteristics of MNWs are shown in Fig. 3(a). The wires were biased with a voltage, ramped from zero with a rate of 0.5 mV/s. Electromigration took place above 0.8 V, and the wires finally

broke at a voltage around 1.2 V. The fact that wires with different resistances broke at a similar voltage indicates that electromigration, rather than Joule heating, is responsible for the observed breaking. A scanning electron microscope (SEM, Hitachi S800) image of one of the broken wires is shown in Fig. 3(b). The gap is barely visible because its length is below the resolution limit of the SEM (5 nm). From the measured tunnel resistance of 2.2 G $\Omega$ , the length of the gap can be estimated<sup>19</sup> to be 1 nm, in agreement with the SEM investigation. Such a small gap has been realized within a wire which is only  $\sim$ 15 nm in width.

In conclusion, chemically modified V<sub>2</sub>O<sub>5</sub> fibers have been successfully employed as an etching mask on top of a thin metal layer. After ion-beam etching and removal of the residual mask, conducting metallic nanowires are obtained. The room-temperature  $I$ - $V$  characteristics are linear with a resistance on the order of 10 k $\Omega$ . Nanogaps were created by breaking the MNWs via electromigration. The presented etching mask technique is expected to be compatible with metals which are sensitive against organic resist layers used in e-beam lithography, like polymethyl-methacrylate (PMMA). For example, the superconducting transition temperature of niobium thin films is known to drastically decrease if the metal is evaporated through a patterned PMMA mask.<sup>21</sup> The presented method can be extended to pattern not only thin metal layers, but also all inorganic and organic materials that can be prepared as homogeneous ultrathin films.

The authors are grateful to U. Waizmann, T. Reindl, and F. Scharfner for technical support. This work was supported by the EU project NANOTCAD (Contract No. IST-1999-10828).

- <sup>1</sup>C. Weisbuch and B. Vinter, *Quantum Semiconductor Structures* (Academic, Boston, 1991).
- <sup>2</sup>S. Datta, *Electronic Transport in Mesoscopic Systems* (Cambridge University Press, Cambridge, U.K., 1995).
- <sup>3</sup>T. Ando, Y. Arakawa, K. Furuya, S. Komiyama, and H. Nakashima, *Mesoscopic Physics and Electronics* (Springer, Berlin, 1998).
- <sup>4</sup>C. Z. Li and N. J. Tao, Appl. Phys. Lett. **72**, 894 (1998).
- <sup>5</sup>S. Washburn and R. A. Webb, Adv. Phys. **35**, 375 (1986).
- <sup>6</sup>R. A. Webb and S. Washburn, Phys. Today **41**, 46 (1988).
- <sup>7</sup>N. Giordano, Phys. Rev. B **22**, 5635 (1980).
- <sup>8</sup>S. Asai and Y. Wada, Proc. IEEE **85**, 505 (1997).
- <sup>9</sup>Y. Zhang, R. H. Terrill, and P. W. Bohn, J. Am. Chem. Soc. **120**, 9969 (1998).
- <sup>10</sup>C. Durkan and M. E. Welland, Phys. Rev. B **61**, 14215 (2000).
- <sup>11</sup>A. Sugawara, T. Coyle, G. G. Hembree, and M. R. Scheinfein, Appl. Phys. Lett. **70**, 1043 (1997).
- <sup>12</sup>D. Natelson, R. L. Willett, K. W. West, and L. N. Pfeiffer, Appl. Phys. Lett. **77**, 1991 (2000).
- <sup>13</sup>A. Thess, R. Lee, P. Nikolaev, H. Dai, P. Petit, J. Robert, C. Xu, Y. H. Lee, S. G. Kim, A. G. Rinzler, D. T. Colbert, G. E. Scuseria, D. Tománek, J. E. Fischer, and R. E. Smalley, Science **273**, 483 (1996).
- <sup>14</sup>A. M. Morales and C. M. Lieber, Science **279**, 208 (1998).
- <sup>15</sup>M. S. Dresselhaus, G. Dresselhaus, and P. C. Eklund, *Science of Fullerenes and Carbon Nanotubes* (Academic, San Diego, CA, 1996).
- <sup>16</sup>W. S. Yun, J. Kim, K. H. Park, J. S. Ha, Y. J. Ko, K. Park, S. K. Kim, Y. J. Doh, H. J. Lee, J. P. Salvétat, and L. Forro, J. Vac. Sci. Technol. A **18**, 1329 (2000).
- <sup>17</sup>J. Livage, Chem. Rev. **190-192**, 391 (1999).
- <sup>18</sup>A. Christou, *Electromigration and Electronic Device Degradation* (Wiley, New York, 1993).
- <sup>19</sup>H. Park, A. K. L. Lim, A. P. Alivisatos, J. Park, and P. L. McEuen, Appl. Phys. Lett. **75**, 301 (1999).
- <sup>20</sup>H. Park, J. Park, A. K. L. Lim, E. H. Anderson, A. P. Alivisatos, and P. L. McEuen, Nature (London) **407**, 57 (2000).
- <sup>21</sup>T. Hoss, C. Strunk, and C. Schönenberger, Microelectron. Eng. **46**, 149 (1999).